Formation of Honeycomb-Patterned Microporous Films Based on a Fluorinated Poly(siloxane imide) Segmented Copolymer

Xue Jiang,[1] Jian Gu,[1] Yan Shen,[2] Shugen Wang,[1] Xiuzhi Tian[1]

[1]*School of Textiles & Clothing, Key Laboratory of Eco-Textile, Ministry of Education, Jiangnan University, Wuxi 214122, People's Republic of China*
[2]*Jiangsu Environmental Monitoring Center, Nanjing 210036, People's Republic of China*

Received 24 November 2009; accepted 9 June 2010
DOI 10.1002/app.33085
Published online 29 September 2010 in Wiley Online Library (wileyonlinelibrary.com).

ABSTRACT: The preparation of honeycomb-patterned microporous films from a soluble fluorinated poly(siloxane imide) segmented copolymer (PSI) by means of water-droplet templating is reported first in this article. The fluorinated PSI was synthesized from 4,4′-(hexafluoroisopropylidene)-diphthalic anhydride, 2,2-bis[4-(4-aminophenoxy)phenyl]-hexafluoropropane, and diamine-terminated poly(dimethyl siloxane) by condensation polymerization. The obtained copolymer had good solubility in chlorinated solvents (chloroform, dichloromethane, and 1,2-dichloroethane), good thermal stability, and a microphase-separated amorphous structure. The effects of the copolymer concentration, atmospheric humidity, and solvent properties on the pattern formation were investigated. The results show that the film fabricated from the copolymer solution with chloroform as the solvent at a humidity of 90% and a concentration of 0.5 g/L had the most regular honeycomb-patterned micropores. We could tailor the pore shape and size by changing the copolymer concentration or the atmospheric humidity. The prepared regular honeycomb-patterned microporous PSI films have potential applications in cell culture and tissue engineering. © 2010 Wiley Periodicals, Inc. J Appl Polym Sci 119: 3329–3337, 2011

Key words: block copolymers; films; macroporous polymers

INTRODUCTION

Highly ordered microporous polymer films have received great interest in recent years because of their potential applications in chemistry, biology, life sciences, and material technology.[1–6] A variety of methods have been developed so far for fabricating various microporous films from different materials.[7–12] Among them, water-droplet templating is a simple and useful technique. One prerequisite for the successful formation of highly ordered microporous films by this means is the use of highly volatile, water-immiscible organic solvents, such as carbon disulfide or chlorinated solvents. As for the mechanism, the formation process of highly ordered microporous films is commonly considered to proceed as follows:

1. Nucleation and growth of water droplets occur on the surface of the polymer solution due to cooling by rapid solvent evaporation
2. The water droplets are trapped in the solution by the surface tension. The polymer precipitates at the solution/water interface and stabilizes the water droplets effectively from coalescence. The stabilized droplets are arranged into well-ordered packing induced by the lateral capillary force and convection currents.
3. After the solvent and water are evaporated completely, the ordered pores are then obtained.

Siloxane polymers principally based on poly(dimethyl siloxane) (PDMS) are important materials because of their unique properties, such as low-temperature flexibility, high thermal stability, low surface energy, lubricity, hydrophobicity, oxidative resistance, significant gas permeability, and good biocompatibility.[13] In particular, the good biocompatibility makes PDMS useful in the areas of tissue engineering and cell culture. Nevertheless, so far, porous films prepared from PDMS with water

Correspondence to: X. Jiang (drjiangxue@yahoo.com) or X. Tian (xzhtian@yahoo.com.cn).

Contract grant sponsor: National Natural Science Fund of China; contract grant number: 20704018.
Contract grant sponsor: The Fundamental Research Funds for the Central Universities; contract grant number: JUSRP10902 and JUSRP10904.

droplets as templates have not been reported. The reasons are mainly the poor film-forming ability and mechanical strength of linear PDMS and the insolubility of crosslinked PDMS in volatile organic solvents, such as carbon disulfide or chlorinated solvents.

Polyimides are well-known engineering plastics with excellent thermal, mechanical, dielectric, and optical properties; they also have good chemical resistance and high dimensional stability.[14] However, polyimides are generally insoluble in common organic solvents and are infusible, which makes them difficult to process unless they are carefully tailored to improve the solubility of these materials in a wide range of polar and nonpolar solvents.

As mentioned previously, improved properties of poly(siloxane imide) segmented copolymer (PSI) over pure PDMS are hoped for, for example, increased solubility, higher thermal stability, and higher mechanical strength; this would make it possible to obtain ordered microporous PSI films with the technique of water-droplet templating.

In this study, a fluorinated PSI was synthesized by condensation polymerization from 4,4′-(hexafluoroisopropylidene)diphthalic anhydride (6FDA), 2,2-bis[4-(4-aminophenoxy)phenyl]hexafluoropropane (BDAF), and diamine-terminated poly(dimethyl siloxane) (SIDA) and characterized by Fourier transform infrared (FTIR) spectroscopy, ^{1}H-NMR spectroscopy, gel permeation chromatography (GPC), thermogravimetric analysis (TGA), and differential scanning calorimetry (DSC). Thereafter, the fluorinated PSI films were first prepared by simple casting under humid conditions. Some influencing factors on the pattern formation, including the solution concentration of the copolymer, the solvent properties, and the humidity of the atmosphere, were investigated.

EXPERIMENTAL

Materials

6FDA (>98%) was purchased from TCI (Shanghai, China) Development Co., Ltd., and was recrystallized from acetic anhydride before use. BDAF (>96%) was also purchased from TCI (Shanghai, China) Development and was dried before use. SIDA (average molecular weight = 900) was obtained from the Shinetsu Co. (Japan). Tetrahydrofuran (THF) were distilled from molten sodium with benzophenone as an indicator until a dark blue color was obtained. 1-Methyl-2-pyrrolidone (NMP) was distilled under reduced pressure over calcium hydride and stored over molecular sieves (4 Å). All of the drying procedures were performed under dry nitrogen gas. The chlorinated solvents, spectroscopy grade, which contained chloroform ($CHCl_3$), dichloromethane (CH_2Cl_2), and 1,2-dichloroethane ($1,2\text{-}C_2H_4Cl_2$), and other reagents, were purchased from Shanghai Chemical Reagent Co. and were used as received.

Copolymer synthesis

Figure 1 outlines the synthetic route to the PSI. Because SIDA does not dissolve in NMP, a cosolvent system is essential. NMP and THF were used as the cosolvents at a volume ratio of 1 : 1. The polymerization procedure was as follows.

A solution of SIDA (0.7202 g, 0.8 mmol) in 3.5 mL of THF was added dropwise to a solution of 6FDA (0.8885 g, 2 mmol) in 8 mL of THF/NMP (1 : 1) under dry nitrogen. The reaction proceeded at room temperature for 24 h, and then, BDAF (0.6221 g, 1.2 mmol) in 3.5 mL was added. The reaction was continued for another 24 h to yield the precursor, poly(siloxane amic acid).

Thereafter, the chemical imidization was carried out with a prescribed volume of pyridine and acetic anhydride (1 : 1) at room temperature for 48 h. Finally, the reaction mixture was then poured into ethanol solution. The precipitate was collected by filtration and dried *in vacuo* at 60°C for 24 h.

Film preparation (on-solid surface spreading method)

We prepared the ordered microporous films of the fluorinated PSI directly by casting the copolymer solutions (50 μL) on glass substrates at room temperature (25°C) in a chamber (programmable constant temperature and humidity testing machine) with a constant relative atmospheric humidity.

Measurements

As for the fluorinated PSI, the FTIR spectrum was recorded on a Nicolet Nexus470 spectrometer (Illinois, USA) in the optical range 400–4000 cm^{-1} by the averaging of 32 scans at a resolution of 4 cm^{-1}. The ^{1}H-NMR spectrum (Germany) was obtained on a Bruker AMX400 NMR spectrometer with hexadeuterated dimethyl sulfoxide as the solvent. GPC analysis was performed with THF as an eluent. TGA was carried out in a TA DSC Q100 calorimeter (America) at a heating rate of 10°C/min in N_2. A TA SDT Q600 analyzing system connected to a cooling system was used to calibrate the glass-transition temperature (T_g). As for the microstructured films of the fluorinated PSI, the surface morphologies were observed by scanning electron microscopy (SEM; Quanta 200, Holland).

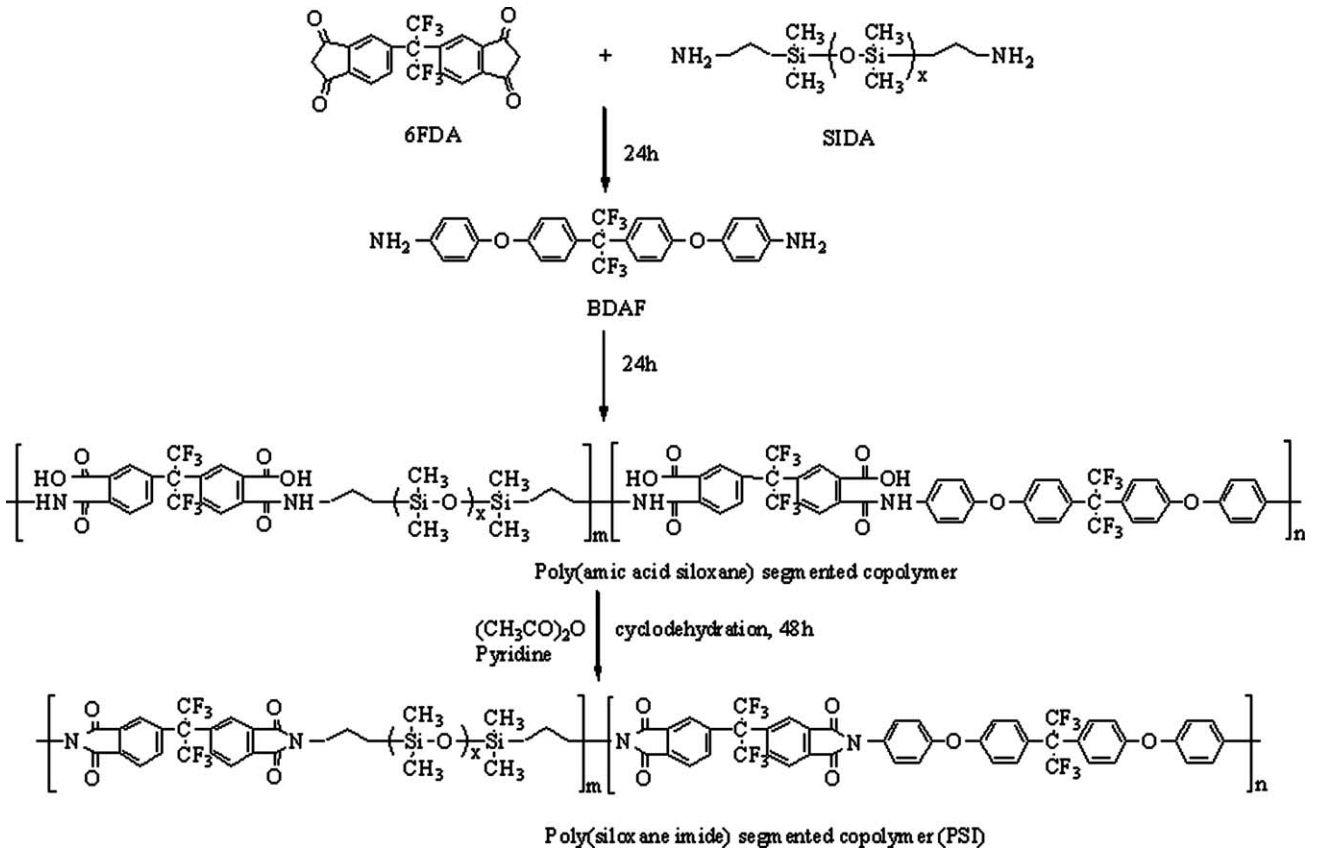

Figure 1 Synthetic route and schematic representation of the fluorinated PSI.

RESULTS AND DISCUSSION

Copolymer characterization

The fluorinated PSI was prepared by the conventional two-step polymerization method, which involved ring-opening polyaddition to form the poly (amic acid siloxane) segmented copolymer and subsequent chemical cyclodehydration to form PSI (Fig. 1). The FTIR spectrum of the fluorinated PSI is shown in Figure 2.

The chemical structure of the copolymer proposed in Figure 1 was verified by the FTIR spectroscopy. The characteristic absorptions for the imide ring (CO_2N) at 1782 and 1723 cm^{-1} due to the asymmetrical and symmetrical carbonyl stretching vibrations, respectively, and that at 719 cm^{-1} due to the ring deformation are clearly shown in Figure 2, whereas those for the amide groups (CO—NH) at 1650–1690 cm^{-1} (I), 1530–1560 cm^{-1} (II), and 1260–1280 cm^{-1} (III) were not detected. Also, those for the N—H in amide and O—H in carboxyl at 2900–3400 cm^{-1} were not observed.[15,16] Hereby, the complete conversion of *o*-carboxyamide groups to the imide rings was thus confirmed.

Other absorptions, which were consistent with the expected copolymer structure, were also distinguished in the FTIR spectrum: Si—O—Si band at about 1010–1100 cm^{-1}, Si—C band at 799 cm^{-1}, aromatic C=C band at 1600 cm^{-1}, C—F band at 1502 cm^{-1}, and aliphatic C—H band at 2962 cm^{-1}.

Moreover, an absence of absorption bands at 3300–3500 cm^{-1} (amine) and 1760–1830 cm^{-1} (anhydride) implied that no unreacted components consisting of BDAF, SIDA, and 6FDA were mixed in the synthesized PSI.

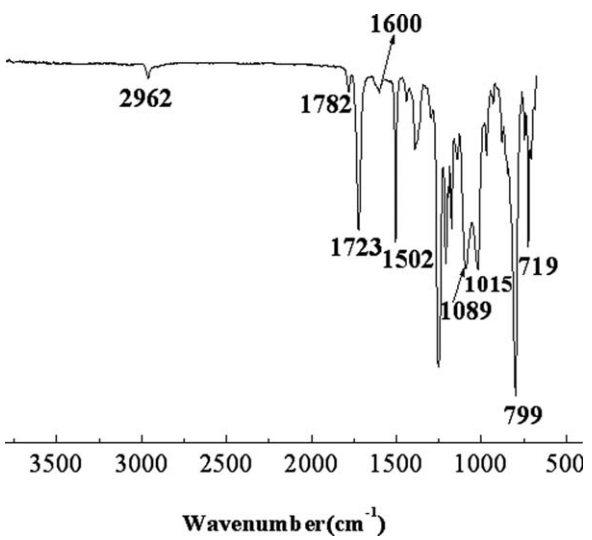

Figure 2 FTIR spectrum of the fluorinated PSI.

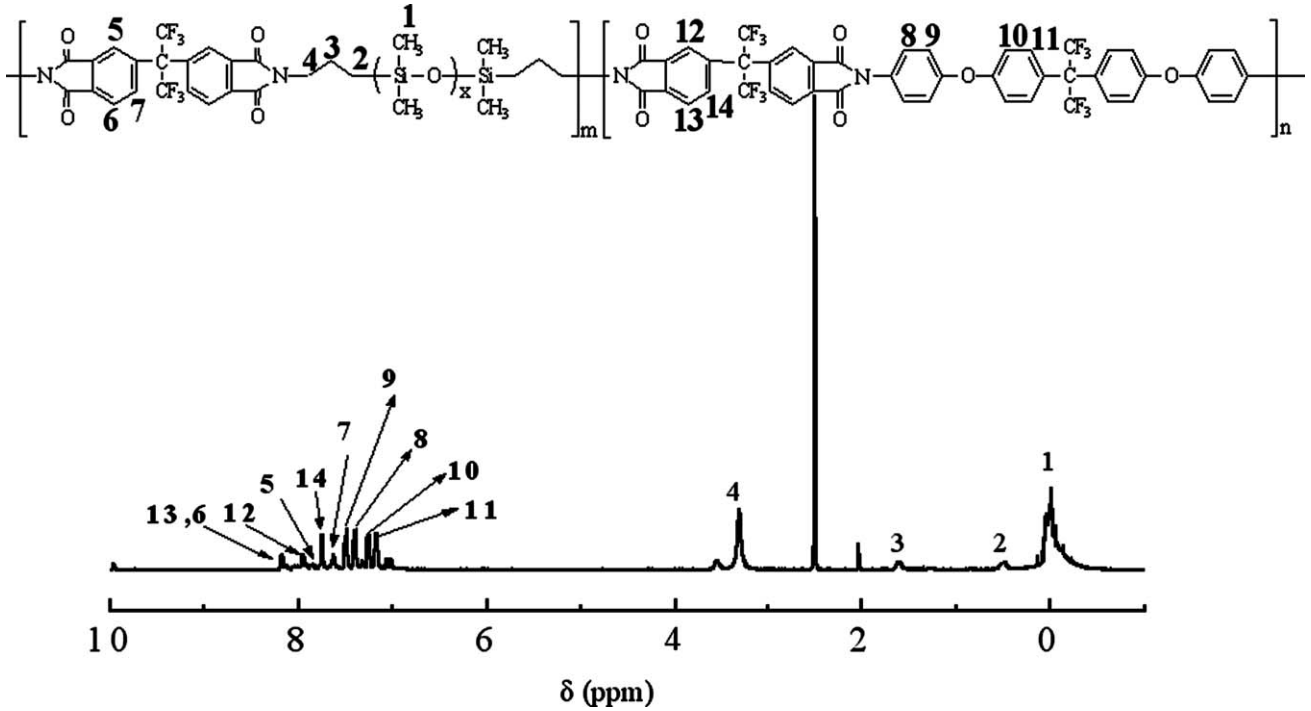

Figure 3 ^{1}H-NMR spectrum of the fluorinated PSI.

The proposed copolymer structure was also confirmed by the chemical shifts in the ^{1}H-NMR spectrum (Fig. 3).

As expected, the aromatic protons were detected around 6.5–8.5 ppm ($H_5 \sim H_{14}$), depending on the position in the aromatic ring.[17] The characteristic peak at 3.6 ppm corresponded to the H_4 protons of the methylene group adjacent to the terminated imide ring (—CH_2—N<). The three other characteristic peaks at about 1.6, 0.6, and 0 ppm corresponded to the H_3 and H_2 protons of the methylene groups and the H_1 protons of the methyl group from the siloxane segments, respectively. As discussed previously, the peaks of all protons in the ^{1}H-NMR spectrum were in good accordance with the proposed copolymer structure. Additionally, no peaks emerged in the range 10–15 ppm; this further validated the full imidization of PSI.

GPC analysis based on linear polystyrene standards gave a weight-average molecular weight of 53,696 and a relatively narrow polydispersity of 1.61 for the fluorinated PSI.

The thermal properties of the fluorinated PSI were characterized with DSC and TGA. The results are shown in Figures 4 and 5, respectively.

As shown in Figure 4, the initial decomposition temperature at about 377°C, the temperature with a 10% gravimetric loss at about 463°C, and also the

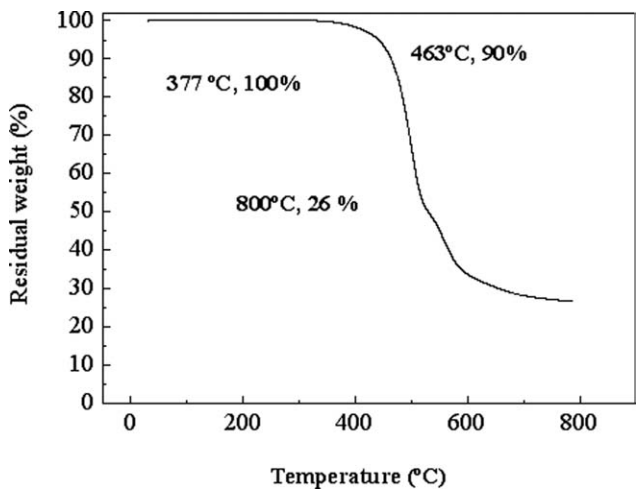

Figure 4 TGA curve of the fluorinated PSI.

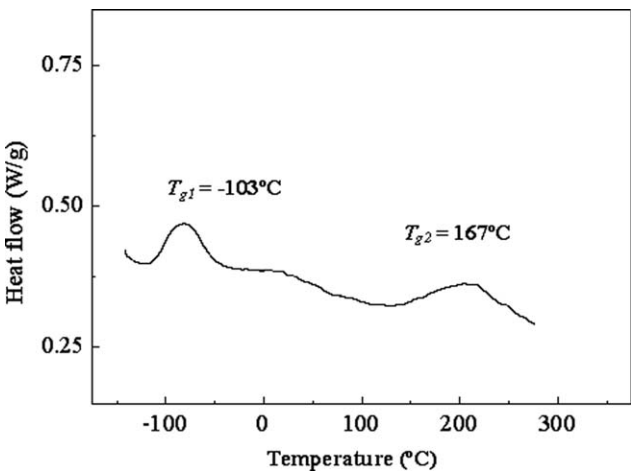

Figure 5 DSC thermogram of the fluorinated PSI.

char yield at 800°C of about 26% demonstrated that the fluorinated PSI had good thermal stability. As also shown in Figure 4, the copolymer containing siloxane units in the polymer backbone underwent a two-step degradation. The first step occurred between 370 and 450°C, which was attributed to the scission of aliphatic amino propyl linkages. The second one occurred between 500 and 600°C and was due to imide group degradation.[18]

As presented in Figure 5, the fluorinated PSI exhibited no crystallization or melting transition in the DSC measurements. However, two glass transitions were observed at −103 and 167°C, each related to the siloxane and imide blocks, respectively. All of these indicated that the fluorinated PSI was almost amorphous but had the microphase separation. The introduction of ether linkages and bulky CF_3 groups in BDAF and 6FDA contributed to a low glass-transition temperature, T_{g2}. However, the higher one, T_{g1}, corresponding to the siloxane block, increased compared with that of pure PDMS (−123°C); this resulted from the limited mobility of the siloxane chains by the rigid imide block.[19]

The solubility was determined with 1 g of the copolymer dissolved in 9 g of the solvent (10 wt %) at room temperature. The fluorinated PSI exhibited good solubility in the polar organic the solvents consisting of NMP, dimethylacetamide, dimethylformamide, dimethyl sulfoxide, THF, and acetone. Besides, it could also dissolve easily in the nonpolar ones with low boiling points, such as $CHCl_3$, CH_2Cl_2, and 1,2-$C_2H_4Cl_2$; this was mainly attributed to the incorporation of bulky —CF_3 groups and ether linkages into the polymer backbone. This good solubility of the copolymer in $CHCl_3$, CH_2Cl_2 and 1,2-$C_2H_4Cl_2$ was the precondition to form regular microporous films by means of water-droplet templating.

Formation and analysis of honeycomb-patterned microporous films

The pore size and its array of honeycomb-patterned films can be easily influenced by the casting conditions, such as the humidity of the atmosphere, polymer concentration, temperature, and airflow.

Influence of the copolymer concentration on the pattern formation

The pore size is considerably influenced by the concentration of surface-active polymer, which stabilizes water droplets, because the concentration determines the total contact area between the water phase and the oil phase.[20] To investigate the influence of the copolymer concentration on the pattern formation, varied concentrations from 0.1 to 5 g/L were applied with the other conditions kept constant, as shown in Figure 6.

The SEM images showed that the most regular honeycomb-patterned micropores formed when the copolymer concentration reached 0.5 g/L. In the case of high copolymer concentration, the formed pores were apt to be round because the surface tension between the water and organic solvent was the main driving force [Fig. 6(e,f)]. When the copolymer concentration was low, the impulsive force of the water droplets was the main driving force; therefore, the pore shape was determined by the arrangement of water droplets and was approximately hexagonal [Fig. 6(b–d)]. The excessively low copolymer concentration led to a low regularity of micropore size and their arrangement because the solution viscosity was too low to encapsulate the droplets or prevent their coalescence; this, consequently, resulted in the formation of disordered films. Herein, at a very low copolymer concentrations (0.1 g/L) in this experiment, the obtained films exhibited a web structure [Fig. 6(a)].[21] On the contrary, an excessively high copolymer concentration led to a highly viscous copolymer solution, and water droplets could not even sink in it because of the resistance before a complete evaporation, which caused a few holes in the films (data not shown).

As also shown in Figure 6, the average size of the pores decreased with increasing the copolymer concentration. This could be explained as follows. According to the commonly accepted formation mechanism of the highly ordered microporous films, the nucleation of droplets on the solution surface and the growth of their size is key to the pore size. The growth rate of nucleons (dR/dt) is proportional to the temperature difference (ΔT) between the atmosphere and the solution surface: $dR/dt \sim \Delta T^{0.8}$. In addition, the relationship between the vapor pressure of the copolymer solution (P), the vapor pressure of the pure solvent (P_0), and the molar fraction of the solute (X_b) agrees with Henry's law [$P = P_0 (1 - X_b)$]. At the nucleation stage, as far as a more concentrated solution was concerned, a lower vapor pressure slowed the solvent evaporation and induced a higher surface temperature.[22] Hence, a lower dR/dt value was acquired because of the smaller ΔT value. On the other hand, the nucleation time was short enough to be regarded as the same for all solutions, so the nucleons of the droplets formed on a more concentrated solution were smaller. At the growing stage, the accelerated process of phase inversion from liquid to solid and the high viscosity of a more concentrated solution limited the growth of the droplets.[23] As discussed previously, smaller pores formed at a higher copolymer concentration.

Influence of the solvent properties on the pattern formation

The solvent is a key factor during the formation of honeycomb patterns. Good compatibility between the polymers and their solvents was necessary for

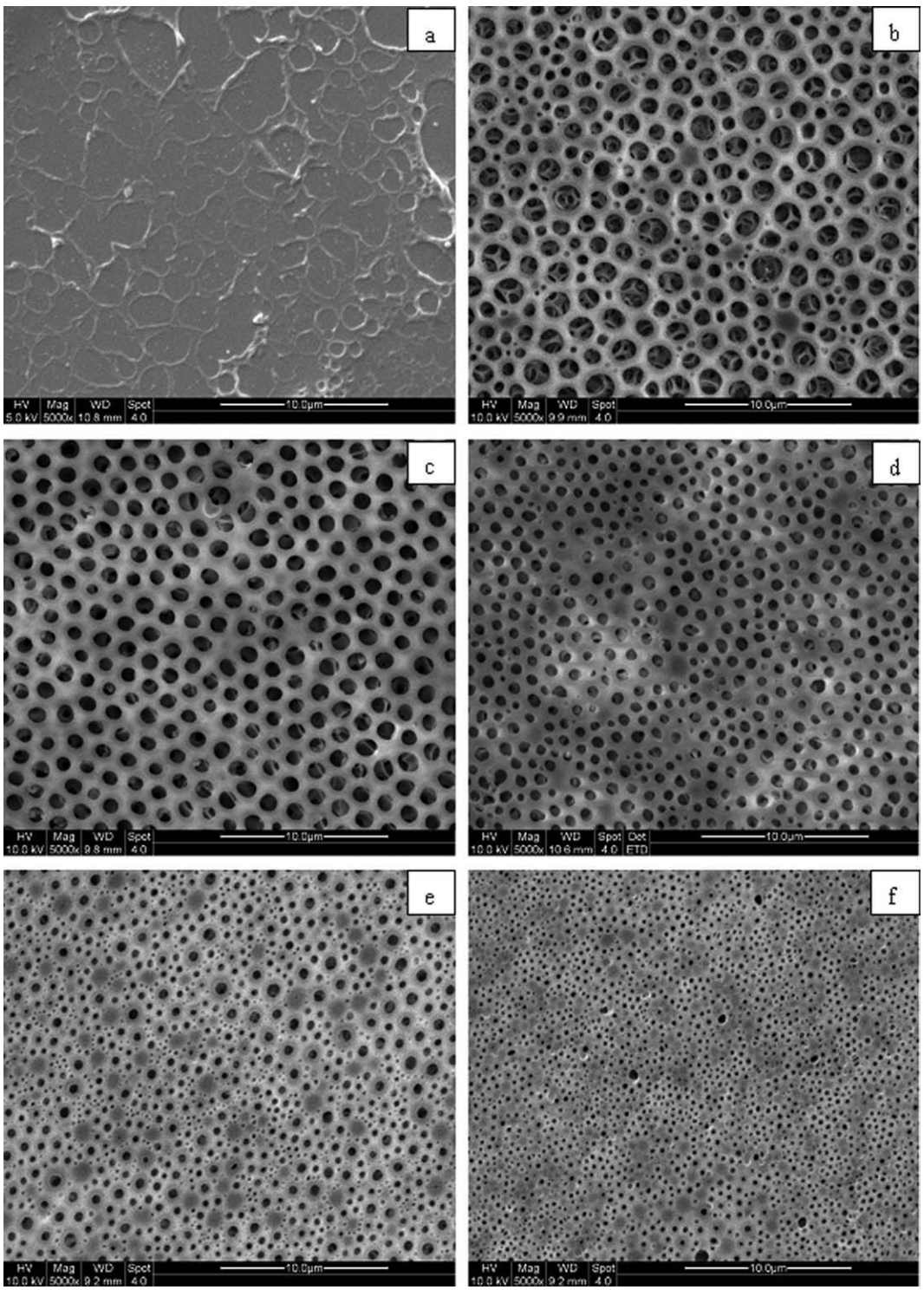

Figure 6 SEM images of the porous structures in the fluorinated PSI films prepared with different casting copolymer concentrations: (a) 0.1, (b) 0.25, (c) 0.5, (d) 1, (e) 2.5, and (f) 5 g/L. The other conditions included $CHCl_3$ as the solvent, a temperature of 25°C, a relative humidity of 90%, and a spreading volume of 50 μL.

the polymer molecules to freely perform Brownian motion in the solution and to stimulate these molecules to aggregate at the interface of the two phases easily; this prevented the water droplets from coalescing and, thereby, gave rise to regular structures. The evaporation rate of the solvent not only influenced the pore size but also the morphology of the honeycomb-patterned films. $CHCl_3$, CH_2Cl_2, and 1,2-$C_2H_4Cl_2$ were good solvents for the fluorinated PSI but had different physical properties (Table I). They were selected to study the influence of the solvents on the pattern formation, as shown in Figure 7.

TABLE I
Physical Properties of the Solvents

	Boiling point (°C)	Molecular weight	Vapor pressure at 20°C (kPa)
CH_2Cl_2	39.8	84.93	46.50
$CHCl_3$	61.2	119.38	21.28
1,2-$C_2H_4Cl_2$	83.5	98.96	8.35

All of the solutions could form porous films, but the patterns and pore size of the holes were evidently different for the three solutions; this explained why the solvents did play a key role in the process of pattern formation.

The evaporation rate was one major difference between the various solvents. Because the evaporation rate depends mostly on the vapor pressure above the liquid and next on the molecular weight of the solvents, usually a higher vapor pressure and lower molecular weight will lead to faster evaporation.[24] CH_2Cl_2 evaporated fastest, and the second fastest was $CHCl_3$, as shown in Table I. As a result, for the PSI/CH_2Cl_2 system, the fast evaporation process of CH_2Cl_2 resulted in a large perturbation of the system in a nonequilibrium state. Under these conditions, the solvent might have disappeared from the system before more water droplets entered the solution surface and formed regular packing. Accordingly, less irregular pores existed in the film, as shown in Figure 7(a). In contrast, 1,2-$C_2H_4Cl_2$ evaporated very slowly, the condensed water droplets had enough time to contact the solvent so that the water droplets acted as nonsolvents for PSI exchanged with 1,2-$C_2H_4Cl_2$ dissolved in water, and a spongy film was thus formed, as exhibited in Figure 7(c). Comparatively, only $CHCl_3$ was suitable for preparing regular honeycomb-patterned microporous films of the fluorinated PSI [Fig. 7(b)] because it evaporated at a moderate rate, and the water droplets, therefore, had time to grow and pack closely on the surface of the solution, which caused the pores to enlarge.

Influence of the atmospheric humidity on the pattern formation

The two-dimensional array of water droplets is a template for the porous structure of the honeycomb film, and the size of water droplets is one of the decisive parameters of the pore size, so the atmospheric humidity influences the water condensation at the air–polymer solution interface and, consequently, influences the pore size and regularity of the micropore arrangement.[12] To investigate the influence of the atmospheric humidity on the pattern formation, the fluorinated PSI was placed into a $CHCl_3$ solution of 0.5 g/L and used to fabricate porous films under different humidities (50, 70, 90, and 95%), with other conditions kept constant, as shown in Figure 8.

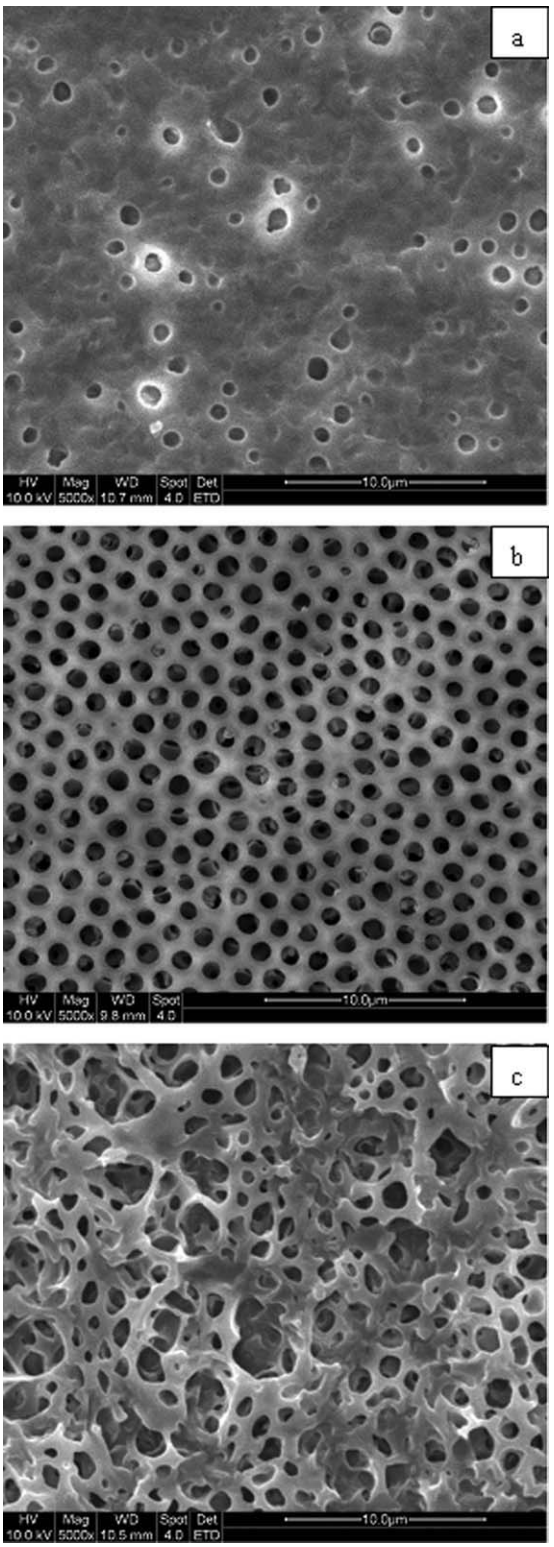

Figure 7 SEM images of the porous structures in the fluorinated PSI films prepared with different solvents: (a) CH_2Cl_2, (b) $CHCl_3$, and (c) 1,2-$C_2H_4Cl_2$. The other conditions included a temperature of 25°C, a concentration of 0.5 g/L, a relative humidity of 90%, and a spreading volume of 50 μL.

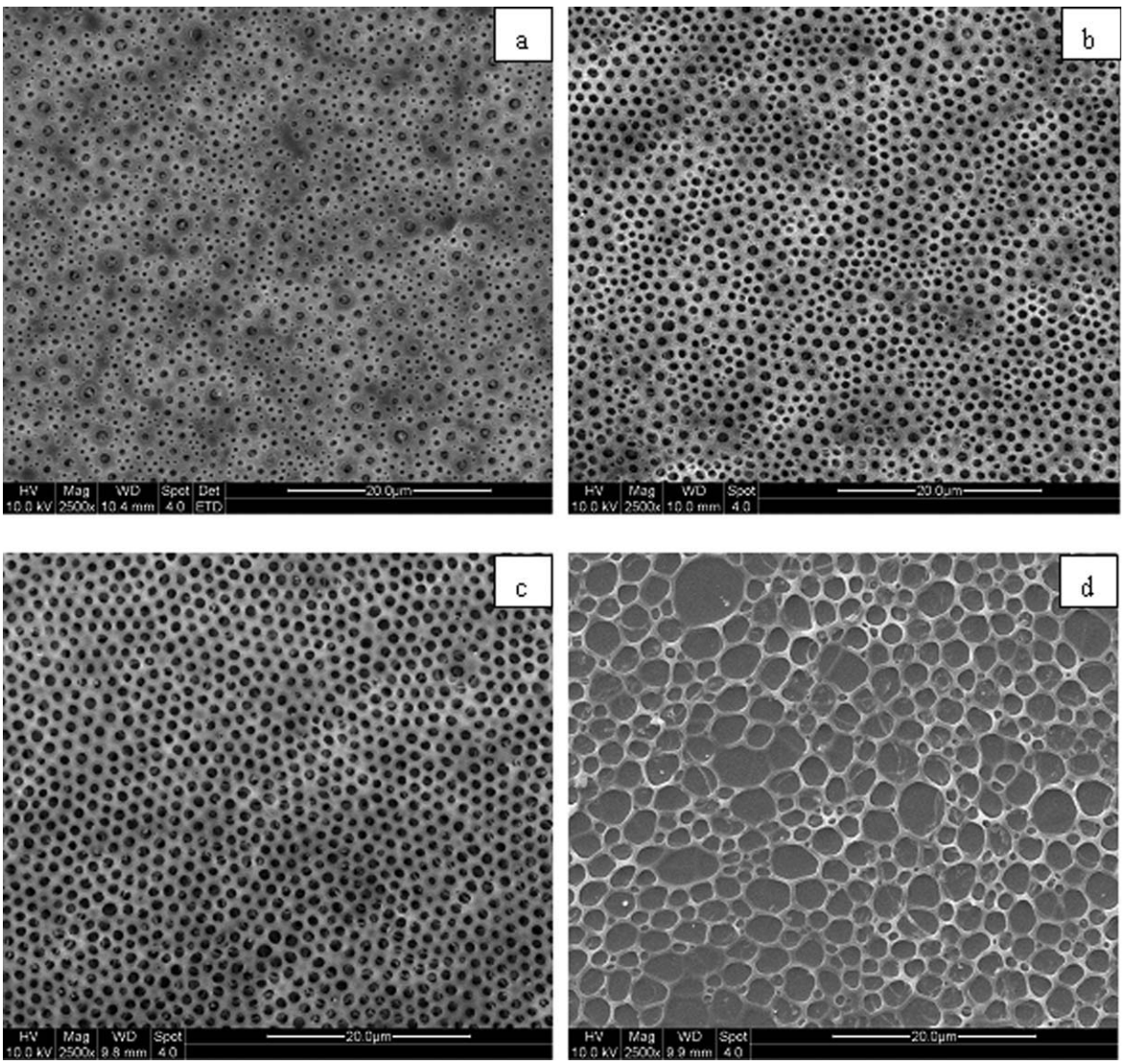

Figure 8 SEM images of the porous structures in the fluorinated PSI films prepared with different relative humidities: (a) 50, (b) 70, (c) 90, and (d) 95%. The other conditions included a temperature of 25°C, a concentration of 0.5 g/L, $CHCl_3$ as the solvent, and a spreading volume of 50 μL.

When the relative humidity was 50%, only tiny pores appeared on the surface of the films [Fig. 8(a)] because, under low atmospheric humidity, no sufficient water droplets were condensed onto the solution surface, and the water droplets were too sparse to arrange in an orderly manner. Regular patterns were found at an increased humidity [Fig. 8(b,c)], so it was safe to say that high humidity was needed to form orderly porous films for such a copolymer. However, when too many water droplets were condensed onto the solution surface under a comparably high humidity (95%), the coalescence of some water droplets could not be avoided; this gave both a larger pore size and also led to a lower regularity of micropore size and their arrangement [Fig. 8(d)]. Otherwise, when the films were fabricated at an excessively low humidity (<50%), the water vapor was condensed to form droplets on the surface of the copolymer solution, and finally, transparent films were induced (data not shown). In general, at a relative humidity of 90%, the regularity of the micropore size and their arrangement were best compared with those at other humidities [Fig. 8(c)].

Moreover, as also shown in Figure 8, the pore size enlarged with increasing humidity. The same result was obtained in other studies.[20]

CONCLUSIONS

To overcome the poor film-forming ability and mechanical strength of linear PDMS or the insolubility of crosslinked PDMS in volatile organic solvents, a new fluorinated PSI was designed and synthesized on the basis of BDAF, 6FDA, and SIDA. The chemical structure of the copolymer was confirmed by FTIR and ^{1}H-NMR spectra. The microphase-

separated amorphous structure and good thermal stability were confirmed by DSC and TGA characterizations. Apart from the segmental copolymerization between siloxane and imide, the introduction of bulky CF_3 groups and ether linkages into the polymer backbone led to an evidently improved solubility of the copolymer, which was even soluble in some chlorinated solvents with low boiling points, such as $CHCl_3$, CH_2Cl_2, and 1,2-$C_2H_4Cl_2$.

The honeycomb-patterned films were first fabricated from the synthesized fluorinated PSI with a water-droplet array acting as a template. Solvents played a key role in the process of pattern formation. Only the copolymer solution with $CHCl_3$ as the solvent could form regular honeycomb-patterned microporous films. We modified the pore shape and size by changing the solution concentration of the copolymer or the atmospheric humidity. The most regular honeycomb-patterned microporous film was fabricated at a relative humidity of 90% and a copolymer concentration of 0.5 g/L. Too low or too high concentration or humidity caused irregular patterns. A higher copolymer concentration or lower humidity resulted in smaller pores.

Together with the good biocompatibility of the copolymer, the regular honeycomb-patterned microporous PSI films prepared by the simple water-droplet-template process in this article have potential applications not only in cell culture substrates but also in scaffolds for tissue engineering.

References

1. Hulteen, J. C.; Jirage, K. B.; Martin, C. R. J Am Chem Soc 1998, 120, 6603.
2. Yabu, H.; Shimomura, M. Langmuir 2005, 21, 1709.
3. Beattie, D.; Wong, K. H.; Williams, C.; Poole-Warren, L. A.; Davis, T. P.; Barner-Kowollik, C.; Stenzel, M. H. Biomacromolecules 2006, 7, 1072.
4. Yabu, H.; Takebayashi, M.; Tanaka, M.; Shimomura, M. Langmuir 2005, 21, 3235.
5. Fukuhira, Y.; Kitazono, E.; Hayashi, T.; Kaneko, H.; Tanaka, M.; Shimomura, M.; Sumi, Y. Biomaterials 2006, 27, 1797.
6. Yabu, H.; Shimomura, M. Chem Mater 2005, 17, 5231.
7. Stenzel, M. H.; Barner-Kowollik, C.; Davis, T. P. J Polym Sci Part A: Polym Chem 2006, 44, 2363.
8. Gamboa, A. L. S.; Filipe, E. J. M.; Brogueira, P. Nano Lett 2002, 2, 1083.
9. Karthaus, O.; Maruyama, N.; Cieren, X.; Shimonura, M.; Hasegawa, H.; Hashimoto, T. Langmuir 2000, 16, 6071.
10. Bolognesi, A.; Mercogliano, C.; Yunus, S. Langmuir 2005, 21, 3480.
11. Nishikawa, T.; Nonomura, M.; Arai, K.; Hayashi, J.; Sawadaishi, T.; Nishiura, Y.; Hara, M.; Shimomura, M. Langmuir 2003, 19, 6193.
12. Cheng, C. X.; Tian, Y.; Shi, Y. Q.; Tang, R. P.; Xi, F. Langmuir 2005, 21, 6576.
13. Srividhya, M.; Madhavan, K.; Reddy, B. S. R. Eur Polym J 2006, 42, 2743.
14. Simionescu, M.; Marcu, M.; Cazacu, M. Eur Polym J 2003, 39, 777.
15. Ghosh, A.; Banerjee, S. J Appl Polym Sci 2008, 107, 1831.
16. Ghosh, A.; Banerjee, S. J Appl Polym Sci 2008, 109, 2329.
17. Wang, L. H.; Tian, Y.; Ding, H. Y.; Liu, B. Q. Eur Polym J 2007, 43, 862.
18. Srividhya, M.; Reddy, B. S. R. J Membr Sci 2007, 296, 65.
19. Yang, H.; Nguyen, Q. T.; Ding, Y. D.; Long, Y. C.; Ping, Z. J Membr Sci 2001, 164, 37.
20. Nishikawa, T.; Ookura, R.; Nishida, J.; Arai, K.; Hayashi, J.; Kurono, N.; Sawadaishi, T.; Hara, M.; Shimomura, M. Langmuir 2002, 18, 5734.
21. Nishikawa, T.; Nishida, J.; Ookura, R.; Nishimura, S.-I.; Scheumann, V.; Zizlsperger, M.; Lawall, R.; Knoll, W.; Shimomura, M. Langmuir 2000, 16, 1337.
22. Xu, Y.; Zhu, B. Z.; Xu, Y. Y. Polymer 2005, 46, 713.
23. Zhao, B. H.; Zhang, J.; Wu, H. Y.; Wang, X. D.; Li, C. X. Thin Solid Films 2007, 515, 3629.
24. Peng, J.; Han, Y. C.; Yang, Y. M.; Li, B. Y. Polymer 2004, 45, 447.